Electronic Supplementary Material (ESI) for Dalton Transactions.

Spin crossover in {Fe(pyrazine)[M(CN)$_4$]} (M = Ni, Pt) thin films assembled on fused silica substrates

Fayan Lai[1], Gábor Molnár[1*], Saioa Cobo[1*] and Azzedine Bousseksou[1*]

[1] LCC, CNRS and Université de Toulouse (UPS, INP), Toulouse, France

Table of contents

1. **^{1}H RMN and IR spectra of {(TBA)$_2$Ni(CN)$_4$}**

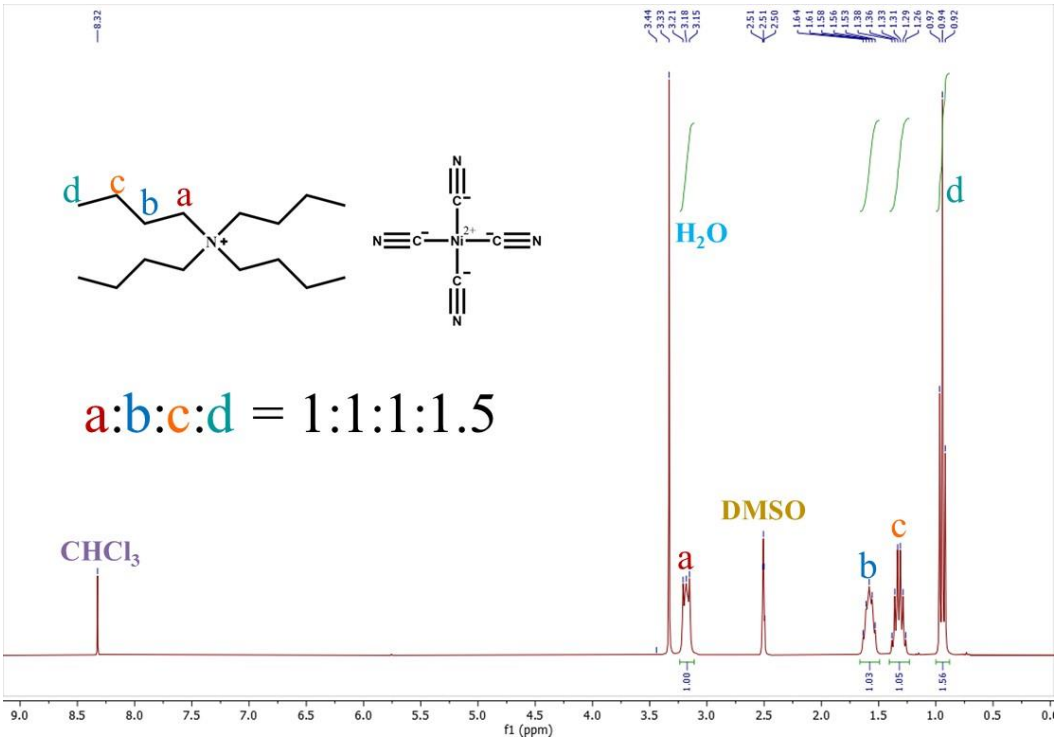

Figure S1. ^{1}H NMR spectrum of {(TBA)$_2$Ni(CN)$_4$}

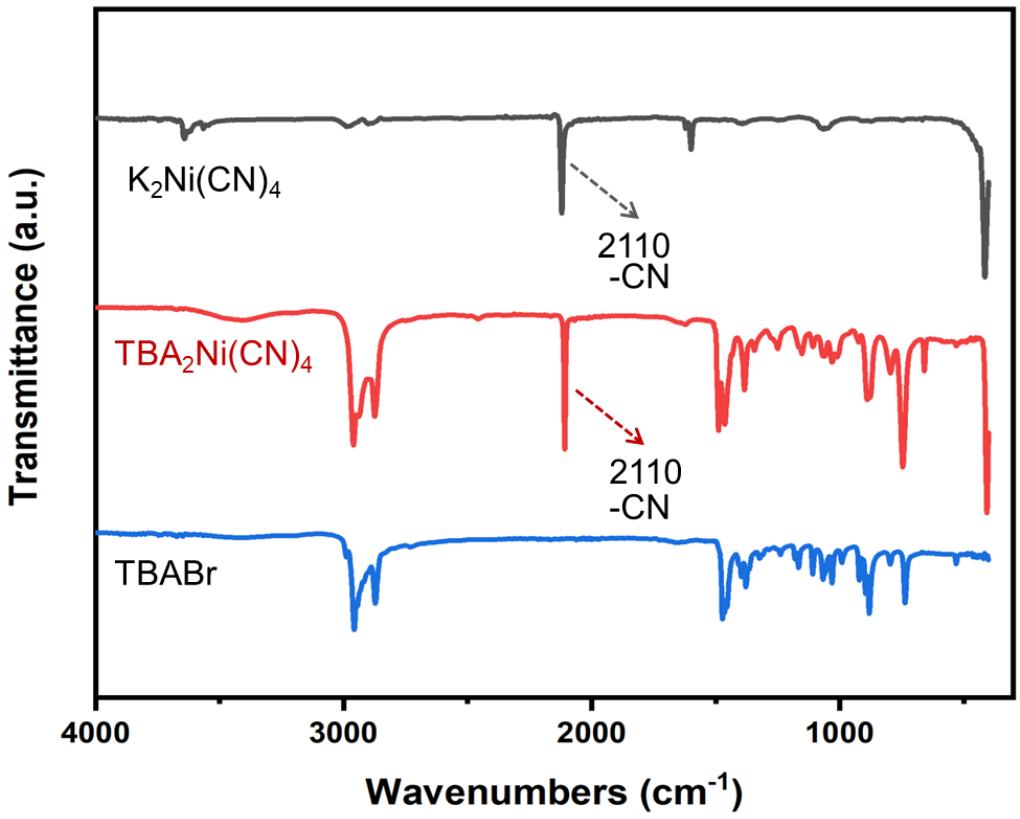

Figure S2. Infrared spectra of {(TBA)$_2$Ni(CN)$_4$}, K$_2$Ni(CN)$_4$ and TBABr

2. AFM images and profiles

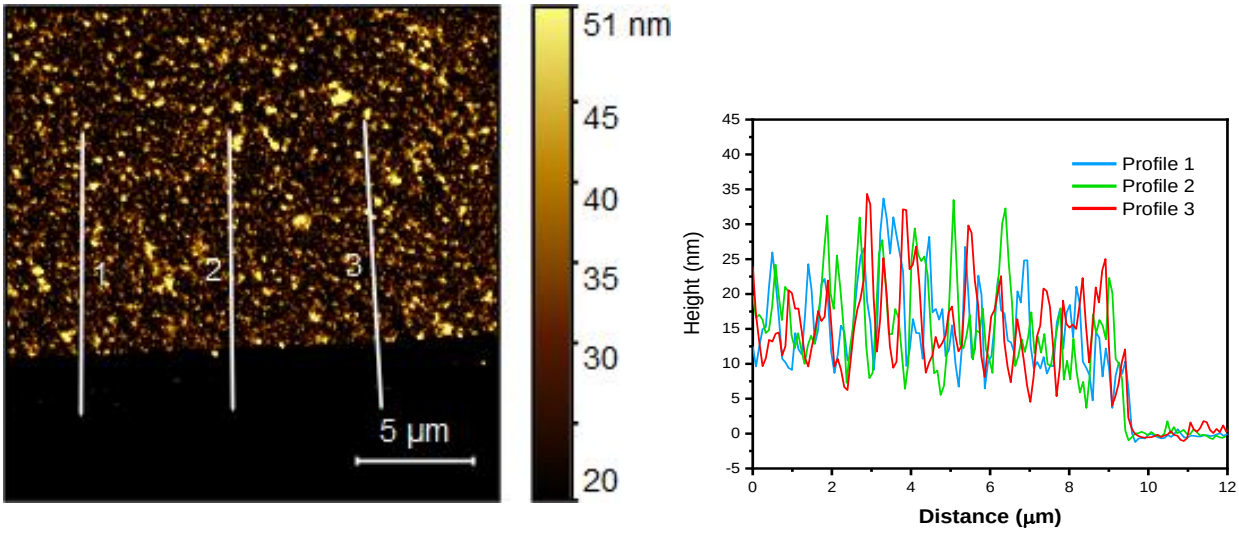

Figure S3. Representative AFM image and cross-sections of a thin film of **1-Ni** following 4 deposition cycles. (Mean Thickness: 14 nm; Mean Roughness: 6 nm.)

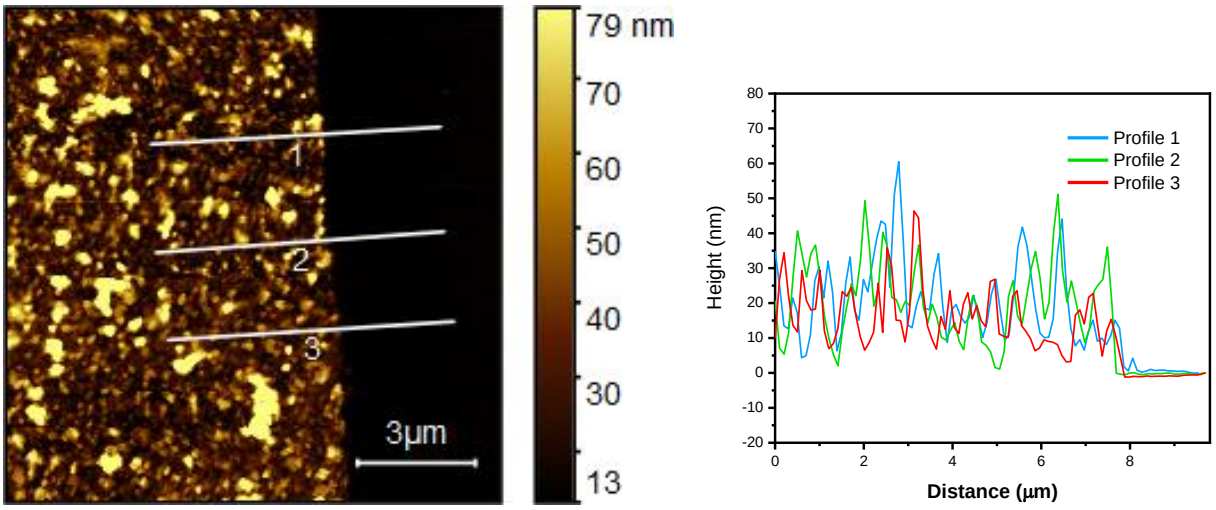

Figure S4. Representative AFM image and cross-sections of a thin film of **1-Ni** following 8 deposition cycles. (Mean Thickness: 25 nm; Mean Roughness: 15 nm.)

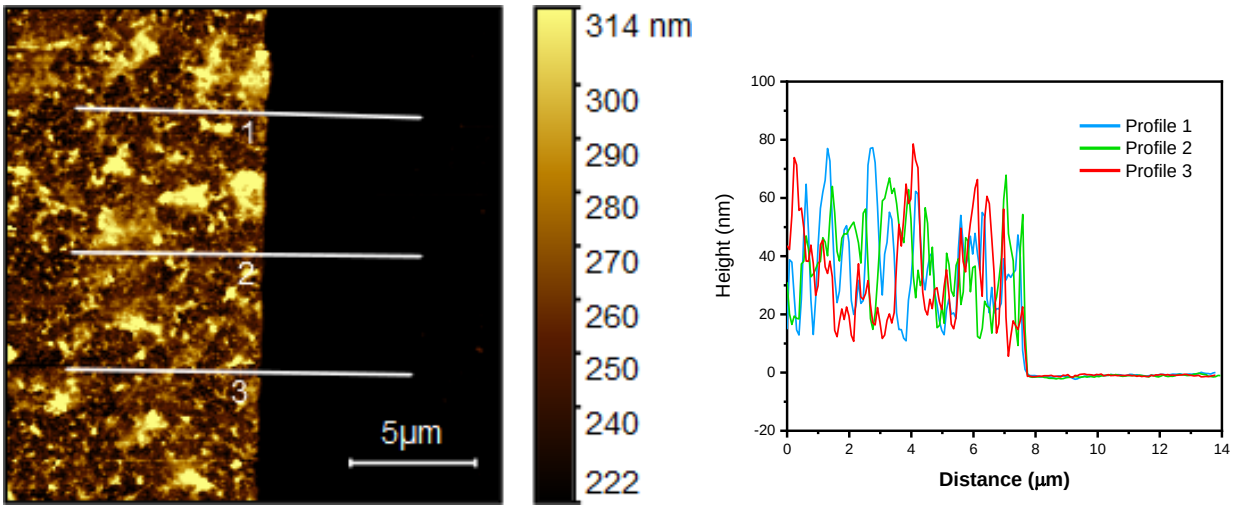

Figure S5. Representative AFM image and cross-sections of a thin film of **1-Ni** following 12 deposition cycles. (Mean Thickness: 36 nm; Mean Roughness: 18 nm.)

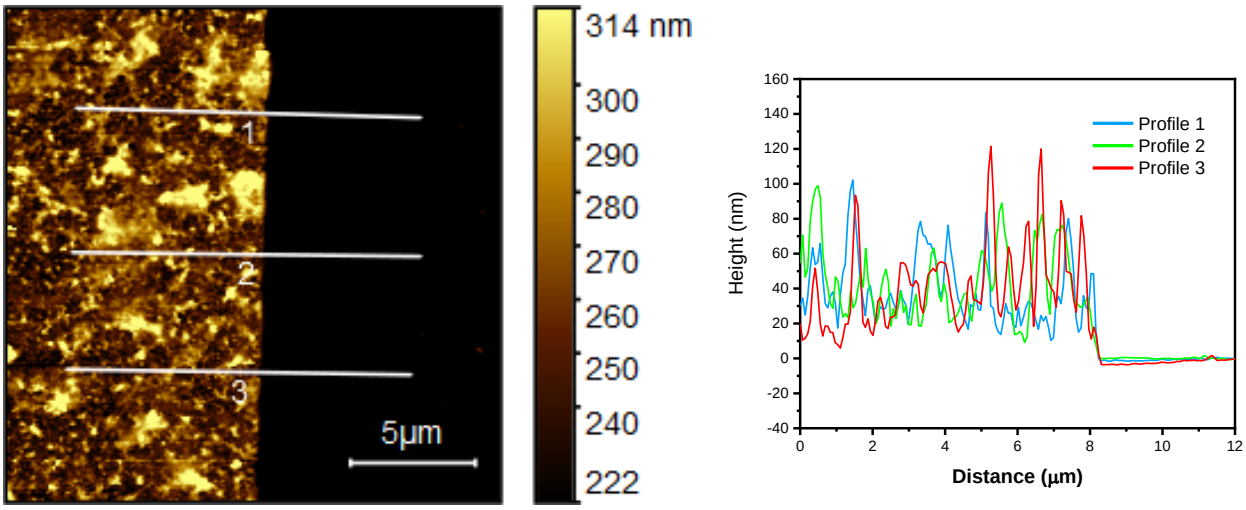

Figure S6. Representative AFM image and cross-sections of a thin film of **1-Ni** following 16 deposition cycles. (Mean Thickness: 40 nm; Mean Roughness: 20 nm.)

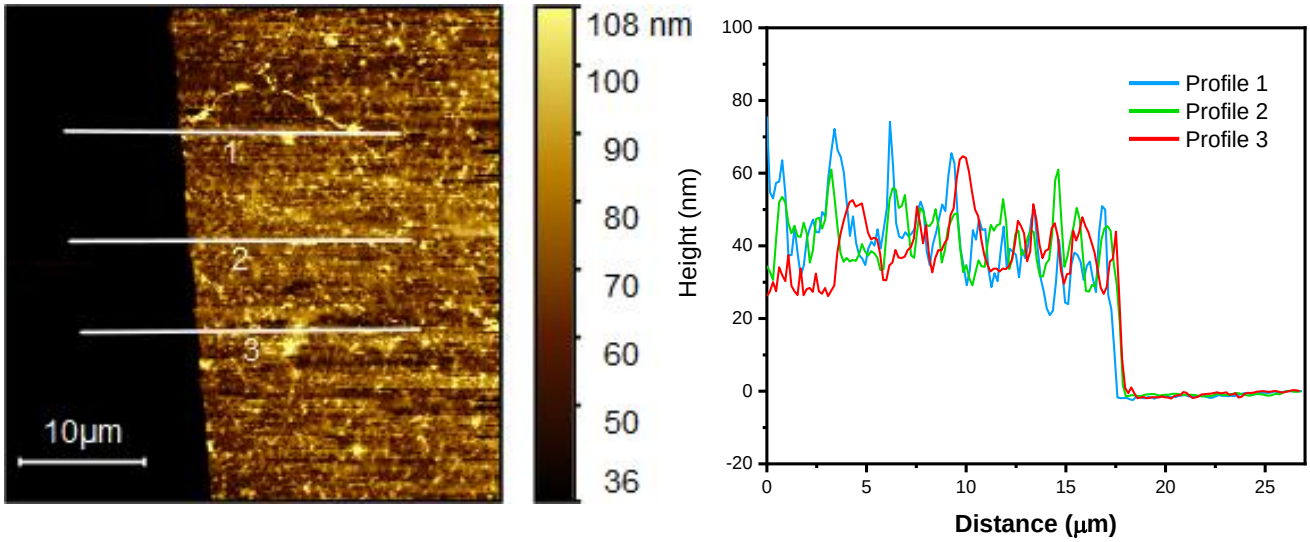

Figure S7. Representative AFM image and cross-sections of a thin film of **1-Ni** following 20 deposition cycles. (Mean Thickness: 46 nm; Mean Roughness: 10 nm.)

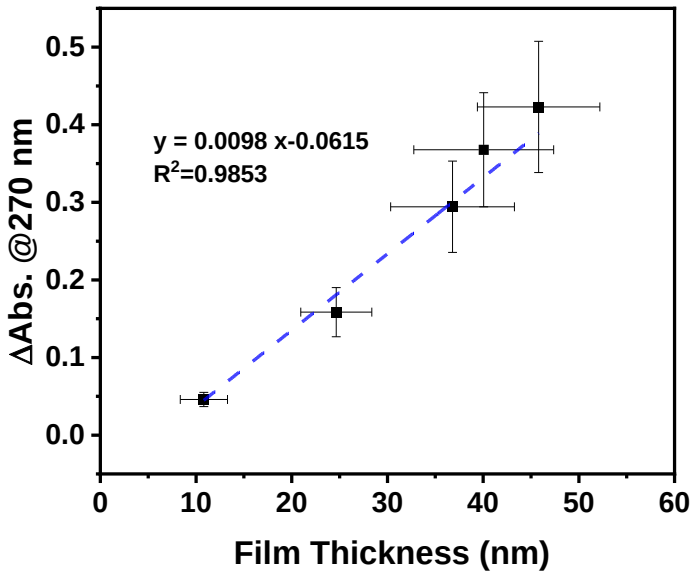

Figure S8. Absorbance at 270 nm vs. film thickness for **1-Ni**. (The film thickness was measured by AFM, the blue dotted line is a visual guide.)

3. Energy Dispersive X-ray analysis

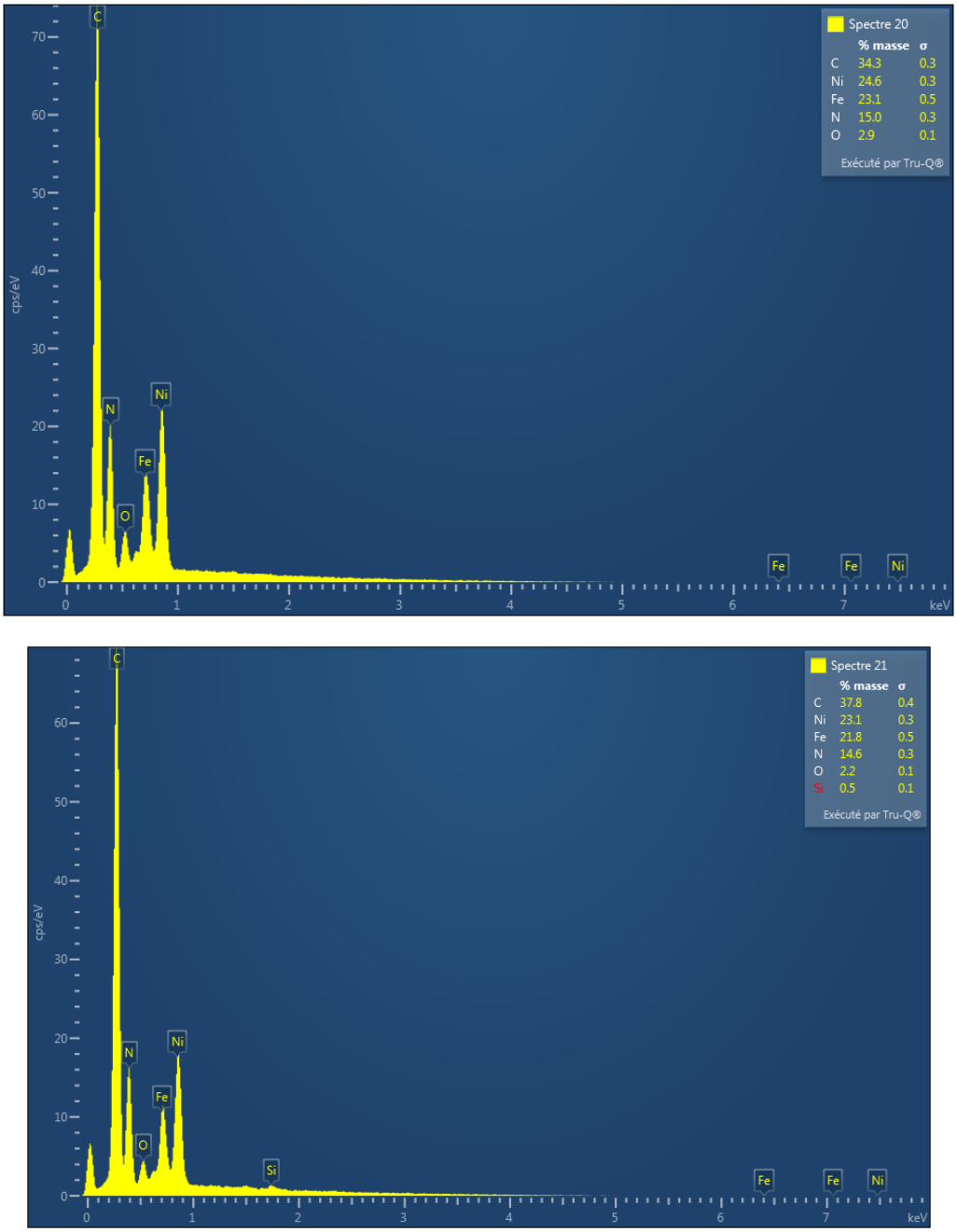

Figure S9: Representative EDX analysis data of a **1-Ni** film (*c* = 50 mM, *N* = 50 cycles).

4. IR and Raman spectra

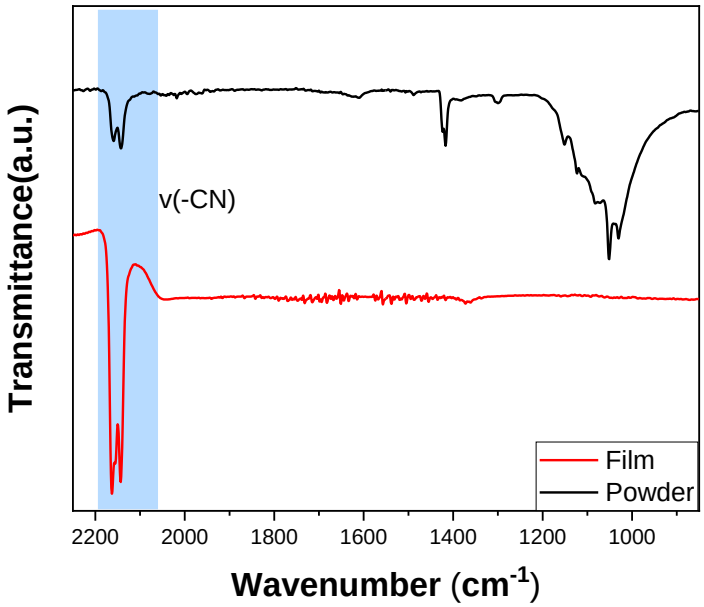

Figure S10. IR spectra of the **1-Ni** powder and thin film (*c* = 50 mM, *N* = 50 cycles). Note that the FS substrate in transmission mode allows only the observation of the CN stretching modes in the film.

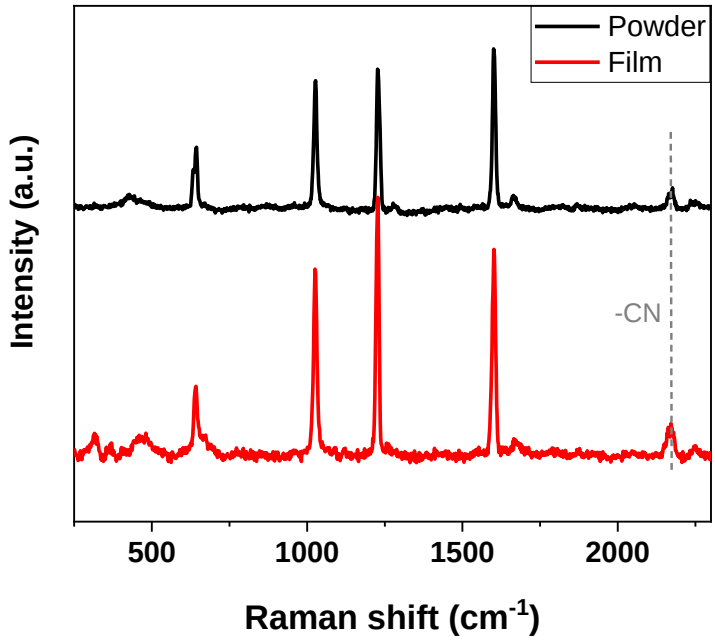

Figure S11. Raman spectra of the **1-Ni** powder and thin film (*c* = 50 mM, *N* = 50 cycles).

5. Effect of the reactant concentration on the fabrication and properties of the films

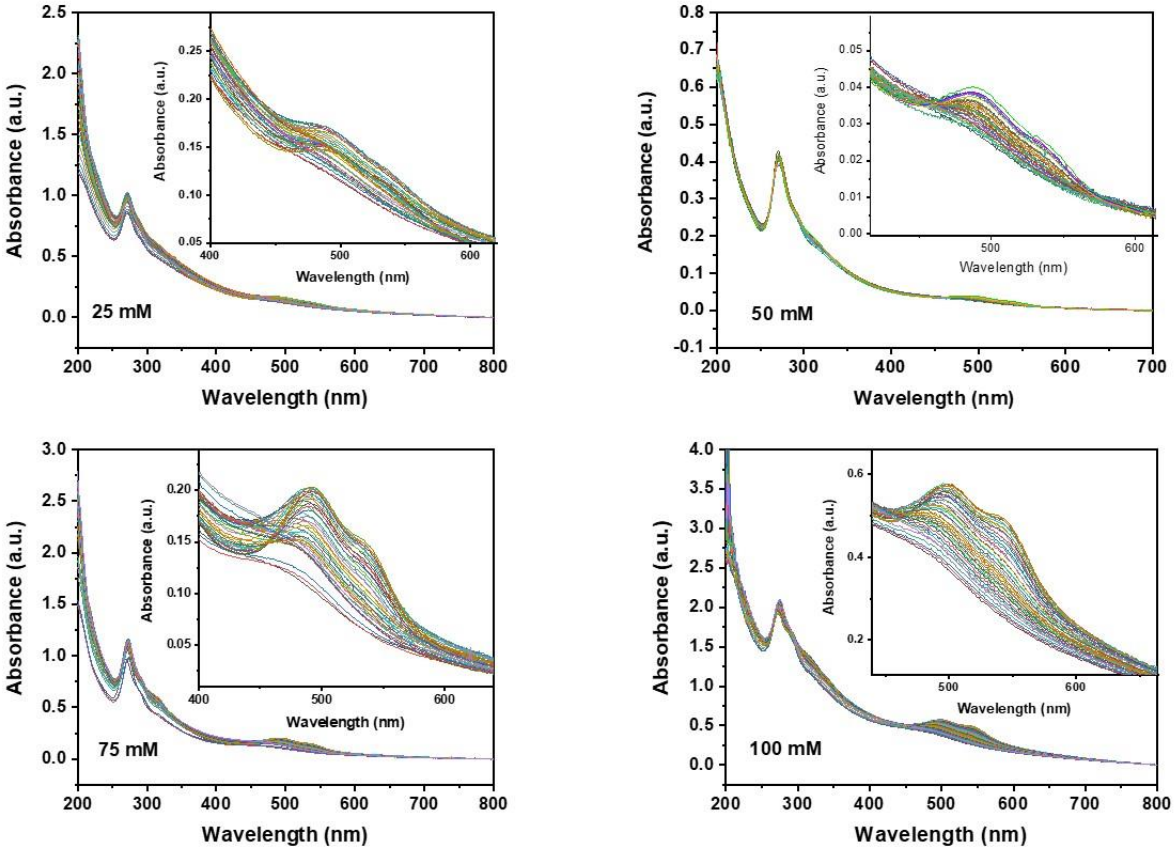

Figure S12. Evolution of a UV–visible absorption spectra of **1-Ni** films recorded upon cooling (*N* = 16 cycles, *T* = 213 K). The films were fabricated at different reactant concentrations (25 mM, 50 mM, 75 mM and 100 mM).

6. Temperature dependence of the absorbance

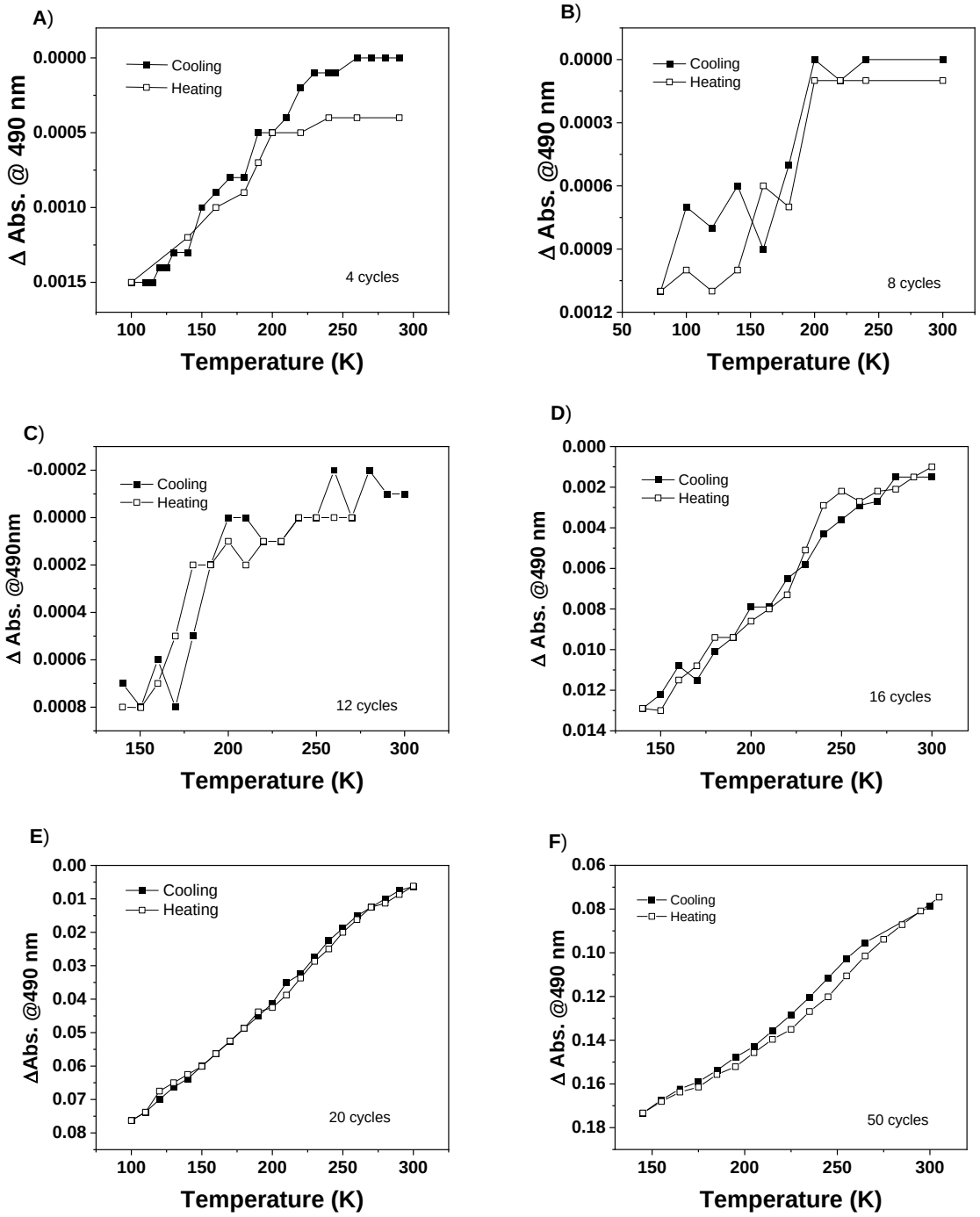

Figure S13. Temperature dependence of the absorbance band intensity at 490 nm of **1-Ni** for A) 4, B) 8, C) 12, D) 16, E) 20 and F) 50 deposition cycles (T = 213 K, c = 50 mM).

7. Grazing incidence X-ray diffraction

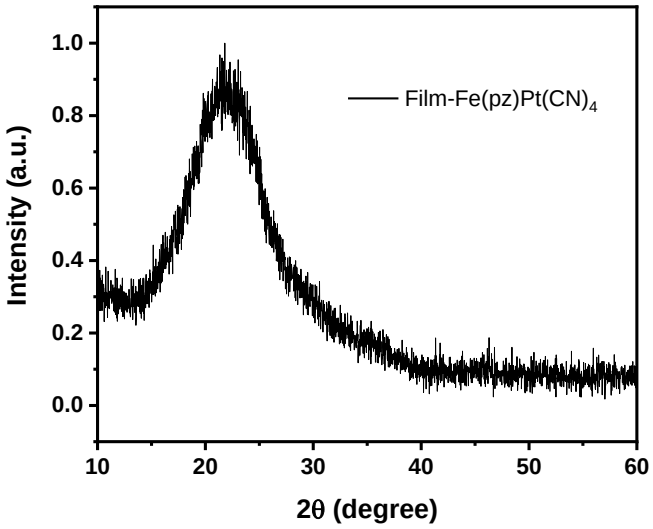

Figure S14. Representative GI-XRD pattern of a film of **1-Pt** for *N* = 16 cycles.